

# Thermodynamics and kinetics of gelation in the poly( $\gamma$ -benzyl $\alpha$ , $l$ -glutamate)–benzyl alcohol system

Premal Shukla

Polymer Physics Program, SRI International, 333 Ravenswood Avenue, Menlo Park, CA 94025, USA

(Received 13 August 1990; accepted 24 October 1990)

Rigid rod-like liquid-crystalline polymers are currently in high demand because of their high modulus and rigidity, and good orientation properties. Gelation is an important phenomenon encountered in lyotropic solutions of polymeric liquid crystals, and this is manifested in fibre spinning and many biological systems. We will focus our attention on the behaviour of gels formed by the synthetic polypeptide, poly( $\gamma$ -benzyl  $\alpha$ , $l$ -glutamate) (PBLG), in benzyl alcohol (BA). More basic than determining the phase boundaries are the questions concerning the definition and identification of the gel phase and the molecular origins of such a phase, along with the added complexity of the dynamics in each phase. In this work, we attempt to make a systematic study of each phase for the PBLG–BA system, using rheological, thermal and light scattering experiments.

(Keywords: thermodynamics; kinetics; gelation; polypeptide; liquid-crystalline polymers)

## INTRODUCTION

The growing demand for high-modulus fibres has resulted in the recent upsurge in the synthesis and production of liquid-crystalline polymers. Rigid rod-like liquid-crystalline polymers are currently in high demand because of their high modulus and rigidity, and good orientation properties. In solution spinning, the polymer solution is extruded through a spinneret and the fibrils are drawn through a bath, called a coagulation bath, wherein gelation occurs. The strength of the fibres depends upon the gelation conditions. Gelation is an important phenomenon encountered in lyotropic solutions of polymeric liquid crystals. Gelation is also an important phenomenon in many biological systems. Also, the phase transitions in gels can be used as actuators for chemical sensors, robots, etc. There are two distinct types of gels. In one, all the crosslinks are chemically crosslinked and hence are permanent. In the other, the junction points are formed by physical entanglements. These physical crosslinks make the gels thermoreversible, with the name suggesting that these gels go into solution on heating and the network is re-formed on cooling. In an attempt to understand the structure and dynamic properties of liquid-crystalline gels, we will focus our attention on the behaviour of gels formed by the synthetic polypeptide, poly( $\gamma$ -benzyl  $\alpha$ , $l$ -glutamate) (PBLG) in the helicogenic solvent, benzyl alcohol (BA).

The problem of ordering of rigid rods in solution was first considered by Onsager<sup>1</sup>. His analysis was valid for low concentrations and was based on the second virial coefficient. He showed that a solution of rod-like particles with hard interactions undergoes a thermodynamic phase transition as the particle concentration is increased. Flory<sup>2</sup> presented a lattice theory of solutions of

semi-flexible polymer chains and predicted a phase diagram consisting of three distinct phases depending upon the temperature and polymer concentration. At sufficiently low polymer concentrations and high temperature, the solution is in the isotropic phase. Between the concentrations, which are referred to as the Robinson A and Robinson B<sup>3,4</sup> points, and at high temperatures, the solution is in the narrow biphasic phase, wherein the isotropic and liquid-crystalline phases coexist. Beyond the concentrations corresponding to Robinson B point and at high temperatures, the solution is in the liquid-crystalline phase. At lower temperatures, all the phases go into the wide biphasic phase, where again the isotropic and liquid-crystalline phases are supposed to coexist. The Flory phase diagram is schematically sketched in *Figure 1*.

There have been extensive experimental studies reported in the literature over the past several decades regarding the phase diagram and the properties of polymer solutions in different phases. Many polymers have been used as models of rigid rod-like polymer. The most commonly used polymer is PBLG in a variety of solvents. Pioneering studies were carried out by Miller *et al.*<sup>5–12</sup> to obtain the phase boundaries for solutions of PBLG in dimethylformamide (DMF) using n.m.r. and microscope measurements. The experimentally observed phase diagram was qualitatively similar to that predicted by Flory for stiff chains. In addition, they observed gelation in the wide biphasic phase contrary to the Flory theory, which predicted isotropic and liquid-crystalline phases coexisting. Miller *et al.*<sup>9,13</sup> also found that for gelation of PBLG in toluene, there is a rapid increase of scattered intensity, while the scattering radius changes little. They believed the origin and nature of the gel phase

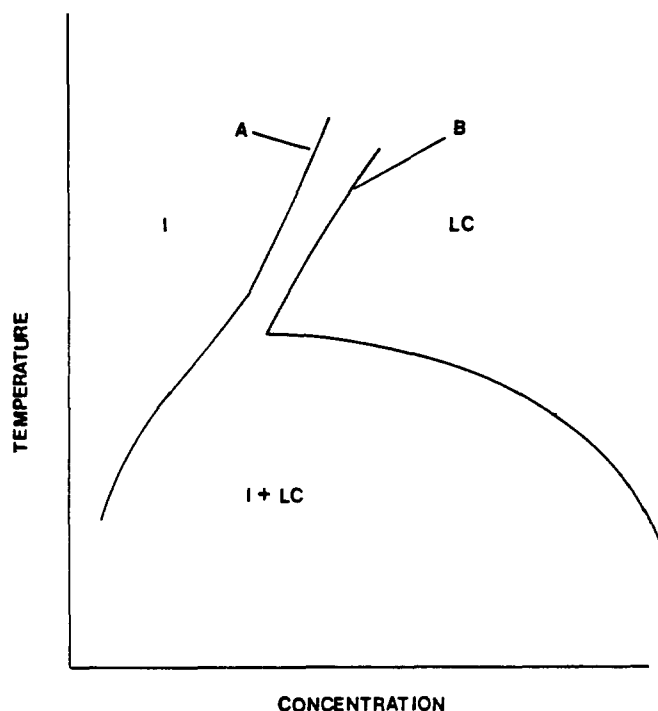


**Figure 1** Typical phase diagram for a rigid-rod polymer solution (not drawn to scale) indicating all the three phases: isotropic (I), liquid crystalline (LC) and biphasic (I + LC). A and B are the concentrations corresponding to Robinson A and B points respectively

to be a kinetic phenomenon, and that the spinodal decomposition mechanism is dominant, leading to bicontinuous interconnected phases that have little possibility or driving force to rearrange further. Effect of side-chain flexibility on the phase equilibria has been included in Flory's theory by Wee and Miller<sup>7</sup>, and later Flory and his coworkers<sup>14–16</sup> incorporated polydispersity in their theoretical model to study its effect on the phase equilibria. Experiments done by Sasaki *et al.*<sup>17,18</sup> and the recent rheological measurements made in our laboratories<sup>19,20</sup> also show that gelation occurs in the wide biphasic region at lower temperatures. It is remarkable that a very dilute solution is able to exhibit gel behaviour when the temperature is reduced by a few degrees.

In an attempt to understand the structure and dynamic properties of liquid-crystalline gels, we will focus our attention on the behaviour of gels formed by the synthetic polypeptide PBLG in the helicogenic solvent BA. In the gel phase formed by stiff chains such as PBLG, the junction points are not permanent crosslinks, but are formed by physical entanglements. These physical crosslinks make the gels thermoreversible, with the gels going into solution on heating and re-forming the network upon cooling. More basic than determining the phase boundaries are the questions concerning the definition and identification of the gel phase and the molecular origins of such a phase. It is of interest to understand the onset, equilibrium and dynamic properties of this gel phase. These fundamental questions and the added complexity of the dynamics in each phase pose considerable difficulties to the successful development of a new theory that can describe the dynamics of such polymers in all phases. In this work, we attempt to make a systematic study of each phase for the PBLG–BA system. Experiments, as well as theory and simulations,

have been used to get a better understanding of the gelation process.

## EXPERIMENTAL

PBLG was purchased from Sigma Chemicals and the solutions were prepared by weighing the polymer and solvent. The concentrations are expressed as weight percentage. The polymer ( $MW = 345\,000$ ; unknown polydispersity; catalogue no. P-5136, lot no. 96F-5013) was dissolved by heating the solution to  $70^\circ\text{C}$  with mechanical stirring.

Oscillatory shear and stress relaxation experiments were performed on a Rheometrics dynamical spectrometer fitted with parallel plates of 25 mm diameter. A polymer solution of a given concentration was poured on the lower parallel plate of the spectrometer, and the upper plate was then lowered slowly until the solution spread evenly between the parallel plates, with sufficient care being taken not to trap any air bubbles in the sample. The plates, which were enclosed in an environmental chamber, were then heated to  $70^\circ\text{C}$  and allowed to stand for 10–15 min. This allows the system to reach thermal equilibrium and ensures loss of any thermal history. It was observed to take several hours for the storage modulus to reach a limiting value, requiring longer times at higher concentrations and lower temperatures. To overcome the time dependence, we followed a fixed time schedule for each temperature. The time required to reach a quasi-equilibrium (2–3 h) value is taken as the fixed time for this temperature, and similarly the times required at all other temperatures were determined. With true equilibrium taking much longer times (days to weeks), this kind of temperature–time schedule allows one to study the system at a stage close to true equilibrium, the only effect being to change the material functions quantitatively, leaving unaffected the qualitative behaviour. Only after reaching a steady value of the storage modulus were experiments carried out.

The small-angle light scattering experiments were performed using a Spectra Physics (2 mW) He–Na laser ( $\lambda = 6328 \text{ \AA}$ ) with a one-dimensional optical multi-channel analyser. The optical system consists of a set of neutral density filters to attenuate the beam and a set of lenses. The combination of lenses determines the scattering angle range to be covered. The scattering pattern is scanned by a vidicon camera, which is connected to a computer for data processing. The sample is held in a glass cell of 1 mm path length. Details about the light scattering set-up can be found elsewhere<sup>21,22</sup>. The angular range was calibrated using a diffraction grating. A simple set-up was used for photographic light scattering. The sample cell was placed in the path of the laser between a polarizer and analyser, and a Polaroid photographic Land film holder was set on top at desired distances to get the scattering patterns. More information can be obtained from our work described in ref. 23.

The dynamic light scattering experiments were performed in the laboratory using a Spectra Physics 165 Ar-ion laser, which provides a beam with a wavelength of  $5145 \text{ \AA}$ , a photomultiplier tube, a pulse analyser/discriminator and LFI correlator model CM-1064. The description of the experimental set-up is given in refs 24 and 25, which should be referred to for details. A block diagram is shown in ref. 24. Samples were inspected for

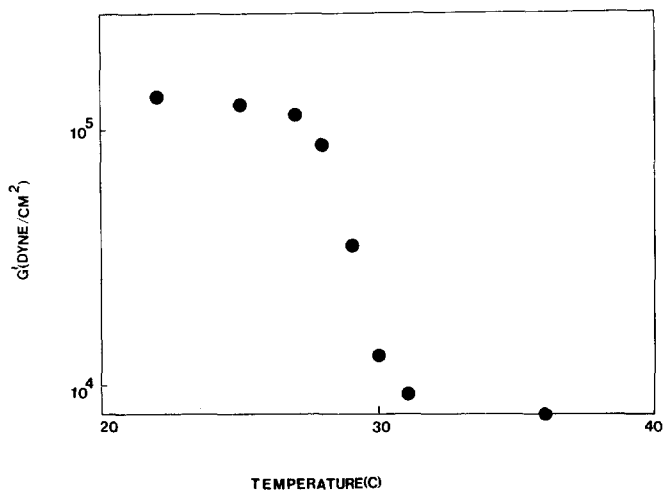


**Figure 2** Dependence of storage modulus ( $\text{dyn cm}^{-2}$ ) increase on the high-temperature phase of the solutions from which gels are prepared ( $\omega = 1 \text{ rad s}^{-1}$ , strain = 1%), from isotropic solution (concentration = 1%) to the gel phase

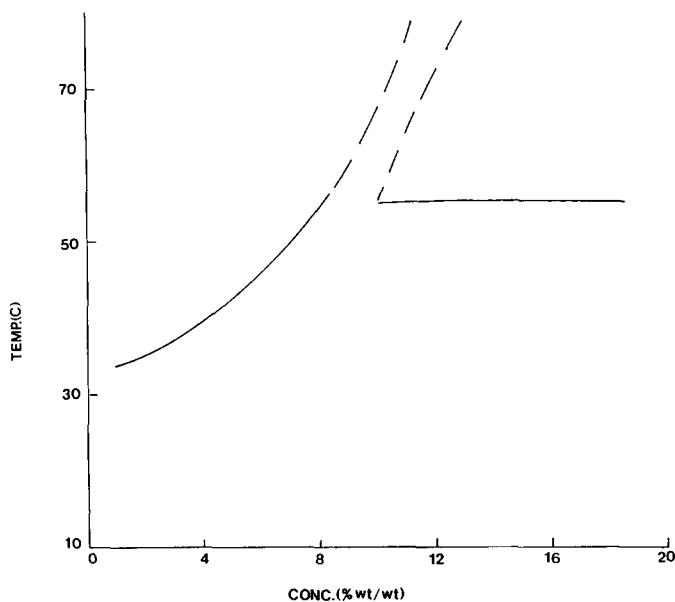


**Figure 3** The phase diagram obtained from the gelation temperature measurements for PBLG-BA solutions ( $MW = 345000$ )

dust using a microscope just ahead of the phototube. Since the microscope lies behind the pinhole, the actual scattering volume can be observed and the presence of dust can be assessed by the eye. The normalized field autocorrelation function  $g^{(1)}(\tau)$  for each sample at a given condition is obtained from the acceptable runs out of 12 attempts. Each run is of duration 20 min and we have used the same criteria as described in ref. 24 to determine the acceptability. We have discussed this in more detail in ref. 25.

## RESULTS AND DISCUSSION

### Oscillatory shear experiments

The gelation temperature was determined by monitoring the gradual build-up of the storage modulus on going from the solution to the gel phase. This change is more dramatic in going from the isotropic to the gel state (i.e.

at low concentrations) than going from the anisotropic cholesteric phase to the gel state (i.e. at high concentrations). Figure 2 shows the dependence of the storage modulus on temperature for 1% concentration solution. This was used to arrive at a phase diagram for this system (Figure 3). The narrow biphasic region at high temperature is shown in broken lines because of the difficulties involved in the precise determination of its phase boundaries.

Very little dependence of  $G'$  and  $G''$  on frequency was observed, and the fact that  $G'$  is higher than  $G''$  at all frequencies indicated the elastic nature of the PBLG solutions in benzyl alcohol. Figure 4 shows the storage and loss moduli and complex viscosity plotted as functions of frequency for a 9% concentration PBLG gel at 28°C and 1% strain. At all temperatures studied, both  $G'$  and  $G''$  show the same frequency dependence, suggesting that the sample retains high-temperature structure even at lower temperatures. The complex viscosity decreases with frequency according to a scaling law,  $\eta^* \sim \omega^{-1}$ . The real component of the complex viscosity,  $\eta' = (G''/\omega)$ , decreases with frequency as  $\omega^{-1}$ , reaching no limiting value at lower frequencies. Apparatus limitations prohibited the use of lower frequencies. The linear viscoelastic regime, at all concentrations and temperatures, is found to be restricted to very small strain levels (up to 3% strain).

The storage and loss moduli increase with concentration up to a certain concentration and then decrease with a further increase in concentration, with a shoulder on the lower-concentration side (Figure 5). This may be an indication of the liquid-crystalline phase dispersed in the isotropic matrix. It is customary to identify the concentration at which viscosity is maximum as the concentration corresponding to the narrow biphasic region in the phase diagram. Starting with the classic work by Hermans<sup>26</sup>, many others observed a peak in shear viscosity and/or dynamic viscosity versus concentration curves<sup>27-30</sup>. Aharoni<sup>29</sup> observed a shoulder to the left of the viscosity maximum for the polyisocyanate-toluene system, while Kiss and Porter<sup>30</sup> noted a shoulder to the right of the storage modulus maximum for PBLG in *m*-cresol.

The qualitative features of the concentration dependence of  $G'$  and  $G''$  are the same for both high and low

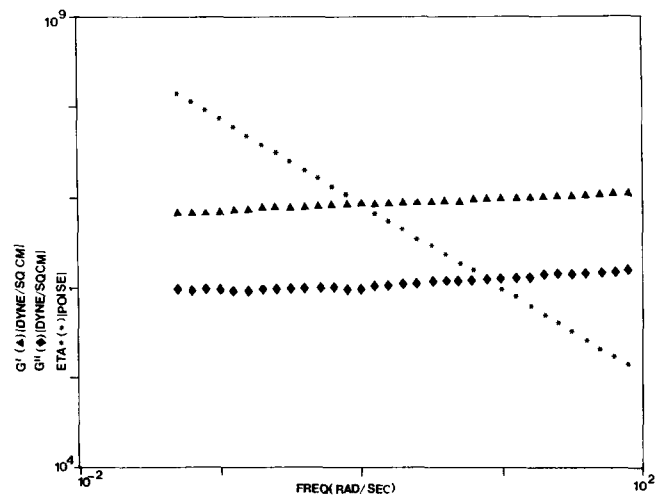


**Figure 4** Storage and loss moduli ( $\text{dyn cm}^{-2}$ ) and complex viscosity ( $P$ ) plotted as functions of frequency, for 9% concentration PBLG gel at 28°C and 1% strain

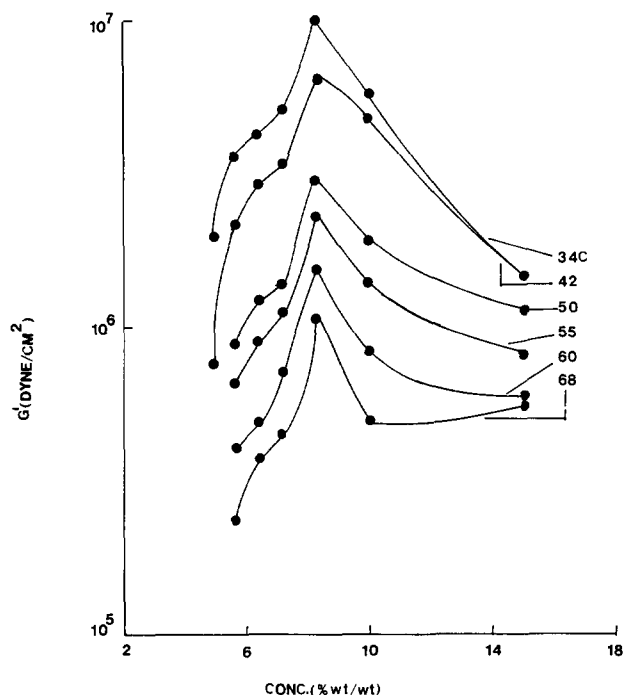


Figure 5 Storage modulus ( $\text{dyn cm}^{-2}$ ) plotted as a function of concentration for different temperatures

temperatures. This demonstrates that the viscoelastic behaviour of the gel state strongly depends on the nature of the high-temperature phase from which the gel phase originated. Also, the viscoelastic behaviour of the gels is time-dependent, and hence kinetically controlled mechanisms dominate the gel behaviour.

#### Static light scattering studies

The light scattering patterns for the PBLG–BA system obtained by depolarized scattering are similar in nature to those found by Hashimoto *et al.*<sup>33–36</sup> for the PBLG–dioxane and PBLG–*m*-cresol systems. The light scattering studies reported here are for PBLG–BA samples in the ordered region, for concentrations greater than 15%. The  $H_V$  pattern was taken with the incident beam vertically polarized and the analyser horizontally polarized. At room temperature, the depolarized pattern is distorted with respect to the azimuthal angle dependence of scattering intensity, the  $H_V$  intensity being greater at azimuthal angle  $\mu = -45^\circ$  than at  $\mu = +45^\circ$ . The  $V_H$  pattern is identical to the pattern obtained by  $90^\circ$  rotation of the  $H_V$  pattern around the incident beam, i.e.  $I_{V_H}(\mu) = I_{H_V}(\mu + 90^\circ)$ , suggesting that the distortion originates from optical activity of the solution, and not because of orientation of cholesteric domains, because in that case the  $H_V$  and  $V_H$  patterns would be distorted in the same direction.

At small scattering angles, we observe optically anisotropic domains randomly oriented in space, which result in the small-angle scattering pattern being angularly dependent with the azimuthal angle  $\mu$ . At larger angles, we observe the cholesteric twisted structure, which exists as an internal structure in these anisotropic domains, and this gives rise to a scattering maximum. The wide-angle scattering maximum corresponds to one-half the cholesteric pitch  $P$ , and the scattering angle of the maximum  $\theta_m$  is interrelated by the Bragg equation,  $2S \sin(\theta_m/2) = \lambda_m$ , where  $S$  is the half-pitch and  $\lambda_m$  is the wavelength of light in the medium<sup>31,32</sup>.

Hashimoto *et al.*<sup>33–36</sup> have published a series of papers on the supramolecular structure of polypeptides in concentrated solutions and films. They have investigated the cholesteric mesophase of PBLG in concentrated solutions of helicogenic solvents (but not in benzyl alcohol). The depolarized elastic scattering indicates the existence of two types of rod-like scattering, with  $\times$ -type (having maximum intensity at odd multiples of azimuthal angle,  $\mu = 45^\circ$ ) and  $+$ -type (having maximum intensity at multiples of  $\mu = 90^\circ$ ) angular distributions. They have also discussed the origin of such rod-like scattering. Analysis of scattering patterns provides information on sense and pitch of cholesteric twisting and form–optical rotation effect.

For a 23% concentration sample, it is clearly seen that the depolarized patterns are distorted in opposite directions, below and above  $118^\circ\text{C}$ , indicating that the sign of  $K$  for this system changes from positive to negative with increasing temperature, and hence the sense of the twist changes<sup>31,32</sup> from right-handed to left-handed in agreement with optical rotation experiments described elsewhere<sup>23</sup>.

Intensity *versus* scattering angle (or scattering vector) plots show a scattering maximum (Figure 6). The location of the scattering maximum  $q_m$  corresponds to one-half the cholesteric pitch  $P$ , and the scattering angle of the maximum  $\theta_m$  is interrelated by the Bragg equation,  $2S \sin(\theta_m/2) = \lambda_m$ , where  $\lambda_m$  is the wavelength of light in the medium,  $S$  is the half-pitch,  $\theta_m$  is the scattering angle of the maximum intensity, and the scattering vector  $q = (4\pi/\lambda) \sin(\theta/2)$ . The position of the scattering maximum first shifts towards smaller angles with increasing temperature up to  $118^\circ\text{C}$ , at which the maximum disappears. With a further increase of temperature, the scattering maximum appears again and shifts towards larger scattering angles. Thus the cholesteric pitch increases with increasing temperature and approaches infinity at  $118^\circ\text{C}$ . The pitch decreases with a further increase of temperature. The inversion temperature is  $118^\circ\text{C}$  for this concentration.

The scattering maximum approaches larger angles as concentration is increased, thus having smaller values of pitch. Also the inversion temperature increases as the concentration is increased. The inversion temperature for 18% conc. solution is  $105^\circ\text{C}$ .

Figure 7 is a plot of the reciprocal half-pitch *versus* temperature for the PBLG liquid crystals in BA, at

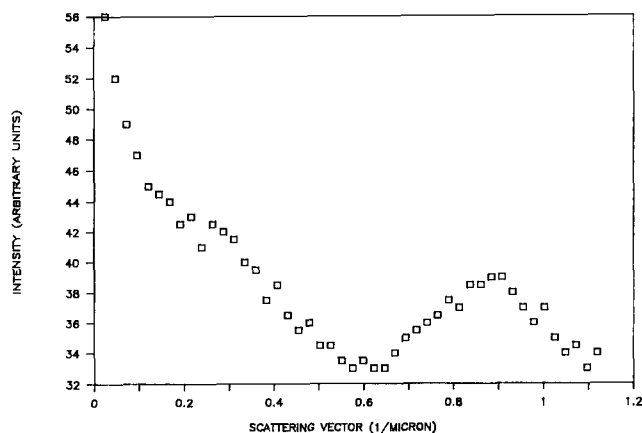


Figure 6 Intensity *versus* scattering vector plot for 23% concentration PBLG–BA system at  $30^\circ\text{C}$

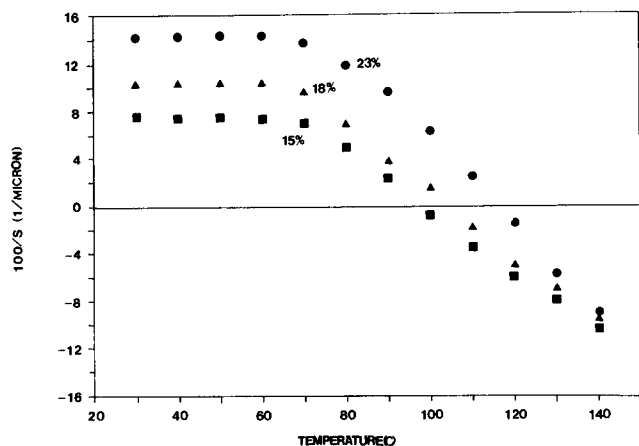


Figure 7 Reciprocal half-pitch versus temperature for different concentration PBLG–BA solutions

different concentrations. The cholesteric liquid-crystalline texture is also observed in the gel phase, and the pitch is maintained in the gel phase. For the 23% concentration solution, the half-pitch  $S$  is nearly constant (about  $6.90 \mu\text{m}$ ) from 30 till about  $65^\circ\text{C}$ , which is the transition temperature between gel phase and the cholesteric phase. Endothermic peaks are obtained in the differential scanning calorimetry curve at  $65^\circ\text{C}$ . The value of  $1/S$  changes almost linearly with temperature above  $65^\circ\text{C}$ . The compensation of the left- and right-handedness occurs at  $118^\circ\text{C}$ . The sign of  $1/S$  is taken positive when the cholesteric sense is right-handed. At the inversion temperature, the mesophase is nematic, because of the presence of the threads characteristic of nematic liquid crystals, as observed by optical microscopy.

A cholesteric liquid-crystalline texture of PBLG–BA is observed by a polarized light microscope in the gel phase, between crossed polars, for concentrated gels. The observed dark and bright fringes in the micrograph reflect the twisting of  $\alpha$ -helical molecules in the cholesteric liquid crystals, with the twisted rod axis  $r$  nearly in the plane of the paper. The optical axis or the helical axis  $d$  is twisted in the domain around  $r$ ; in a bright region  $d$  is perpendicular to  $r$  and in the plane of the paper, and in a dark region  $d$  is perpendicular to the plane of the paper<sup>33</sup>. The spacing  $S$  between the successive fringes corresponds to half the cholesteric pitch  $P$ . The symmetry axis of the twisted superstructure changes direction in a continuous manner throughout the sample.

Optical microscopy studies in the pure liquid-crystalline phase exhibit uniform black and white striations. However, as the solution is cooled below the phase boundary in the gel phase, the uniformity of the liquid-crystalline striations is broken by opaque aggregations, which seem to freeze the twisted arrangement of the cholesteric liquid crystals. The symmetry axis of the twisted superstructure changes direction in a continuous manner throughout the gel sample<sup>23</sup>. It is possible that, upon crossing the phase boundary, certain dynamic processes are taking place resulting in a flow of the system, and possible separation of the dilute and concentrated ordered regions. However, just after this separation starts to happen, the concentration in the polymer-rich phase gets too high, inhibiting further separation. At this point, we do see the liquid-crystalline striations, frozen in the aggregate, but they are not uniform, and change direction continuously in the gel

sample. Since the cholesteric liquid-crystalline texture is also observed in the gel phase, and the pitch is maintained in the gel phase, it appears that the twisted arrangement of molecules in the cholesteric phase is frozen by the local molecular aggregation upon gelation.

#### Differential scanning calorimetry

D.s.c. studies were also done on the PBLG–BA system. At lower concentrations, for isotropic solutions, a single peak appears around  $58$  to  $62^\circ\text{C}$ , with a low latent heat. At higher concentrations, beyond 15 wt%, in the ordered phase, two peaks appear in the thermogram. These are due to formation of various types of aggregates. A plot of latent heat of melting versus concentration shows a sharp increase on going from the disordered to the ordered region. In the PBLG–BA system, a small latent heat exists and is endothermic for conversion of the isotropic phase to the liquid-crystalline phase. Consequently, it must be stabilized by entropic considerations. D.s.c. measurements at high temperatures for solutions in the ordered region<sup>23</sup> indicate a transition peak around the temperature where there is a change in the sense of twisting from right- to left-handedness as observed by light scattering and optical rotation experiments.

D.s.c. analysis of dilute gels shows only one peak, thereby indicating the presence of only one type of aggregate. D.s.c. studies of concentrated gels show two transitions on heating (in the ordered region, only one in the isotropic region), but only one on cooling (the lower one). The higher one is sensitive to kinetics, so that it vanishes on repeated heating. This may be due to a crystal phase associated with the PBLG molecules alone. D.s.c. is monitoring the melting of the crystallites, and it is these junction points that make up the junction points of the gel. However, these crystallites are so small that they are below the resolving power of the optical microscope.

Electron microscopy studies<sup>17,37</sup> on dilute PBLG–BA gels (0.5 to 1%) show the presence of an interconnected fibrillar structure, with the fibrils about  $100 \text{ \AA}$  in diameter. Also, inhomogeneities were observed on a larger scale (1 to  $5 \mu\text{m}$ ) with spaces between the aggregates with few polymer chains present.

#### Dynamic light scattering studies

A detailed description of this work has been presented in ref. 25. Consider a PBLG–BA solution with the polymer concentration of 1%. The experimentally measured normalized field autocorrelation function  $g^{(1)}(\tau)$  is presented in Figures 8 to 10, as a function of time for different temperatures. The correlation function in these figures is normalized to the first channel after baseline subtraction.

At high temperatures such as  $70^\circ\text{C}$  (Figure 8),  $g^{(1)}(\tau)$  is decaying monotonically with time.  $g^{(1)}(\tau)$  cannot be fitted to a single exponential and the procedure described in the preceding section is followed in obtaining the transport coefficients. As the temperature is lowered towards the gel point ( $\approx 32^\circ\text{C}$ ), the correlation function exhibits a damped oscillatory decay, as shown in Figure 9. This pattern appears suddenly with a decrease in temperature of about  $1^\circ\text{C}$ , and we take the gelation temperature to be the temperature at which the oscillatory behaviour sets in. At temperatures below the gelation temperature ( $\approx 25^\circ\text{C}$ ), the correlation function

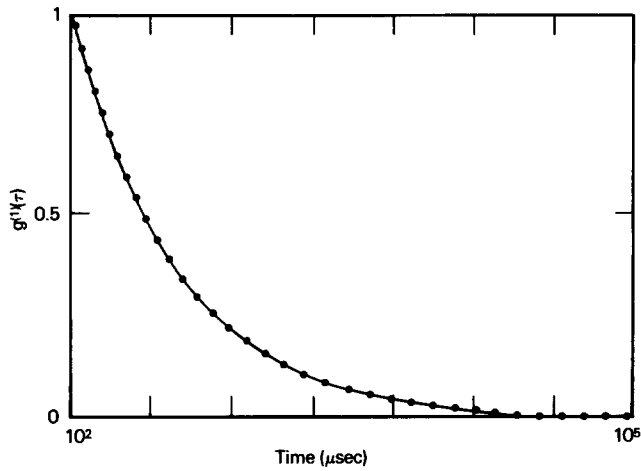


Figure 8 A typical normalized baseline subtracted correlation function at low concentrations and above the gel temperature

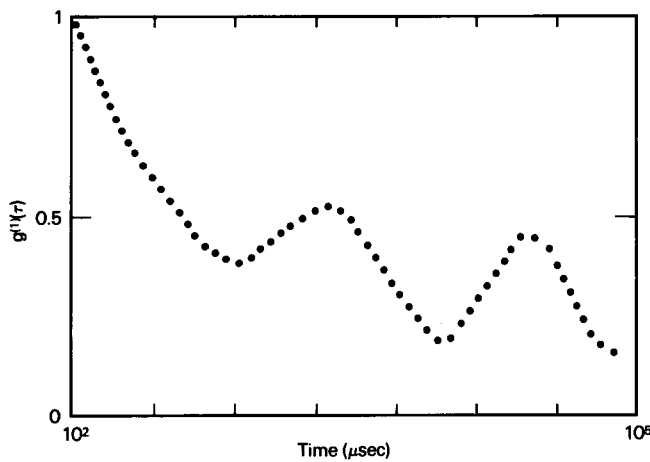


Figure 9 Typical correlation function at the gel temperature

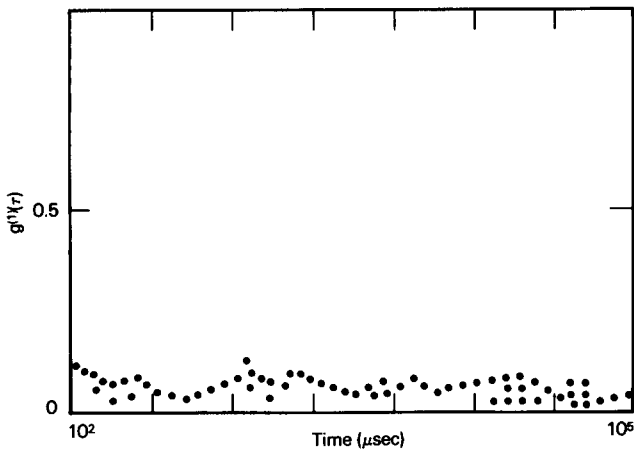


Figure 10 Typical correlation function well below the gel temperature

is essentially independent of time as shown in Figure 10. The damped oscillatory decay of Figure 9 actually persists for only about 3 h and essentially settles into the pattern of Figure 10 although the temperature is maintained constant, indicating the kinetic nature of the formation of the gel phase. The decay pattern of Figure 9 for temperatures near the gel phase is similar to that reported already by Pines and Prins<sup>38</sup> for other aggregating systems.

Accompanying the change in the nature of  $g^{(1)}(\tau)$  as the temperature is lowered, there is also a tremendous change in the scattered intensity. On entering the gel phase, the scattered intensity appears to diverge. The temperature at which this happens obviously depends on the polymer concentration. The temperature dependence of the scattered intensity at various polymer concentrations is given in Figure 11. In an attempt to understand the nature of the gelation process, we have monitored the time dependence of the scattered intensity after a temperature quench. A 5% concentration sample is quenched from 70 to 25°C within 2 s, and the time evolution of the scattered intensity is shown in Figure 12. The observed growth in intensity with time is indicative of an aggregation process and is not consistent with the mechanism of spinodal decomposition. In fact the data of Figure 12 for times greater than  $t_0$  can be fitted to the empirical Avrami equation with Avrami exponent of  $\sim 1.5$ , indicating the diffusion-controlled fibrillar formation as the mechanism of aggregation.

### PROPOSED MECHANISM OF GELATION

#### Dilute gels

In dilute solutions, at high temperatures in the isotropic solution, the PBLG stiff chains are randomly

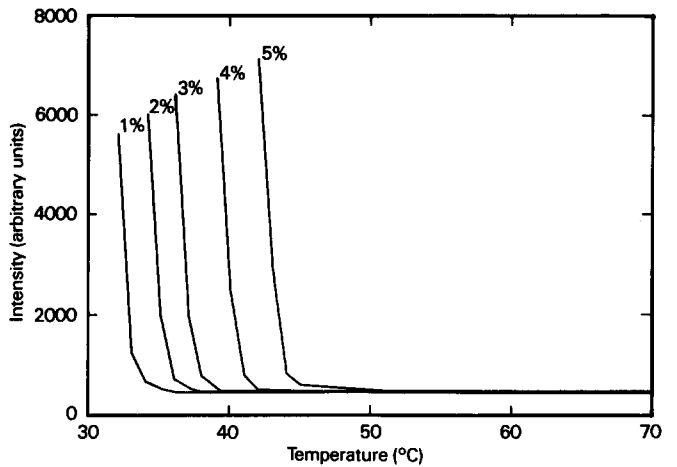


Figure 11 Plot of intensity versus temperature for different concentration PBLG-BA solutions

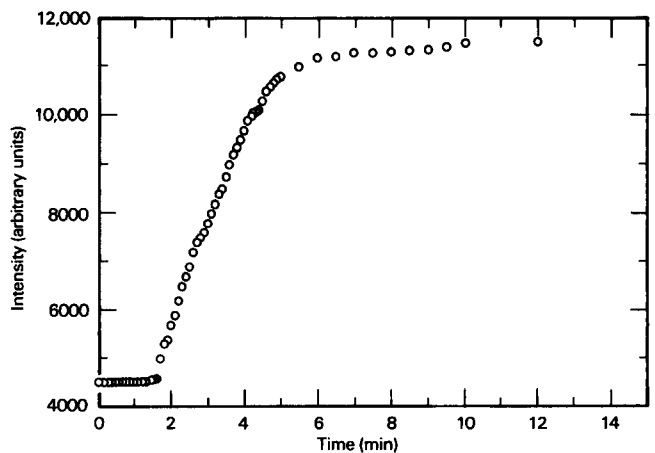


Figure 12 Plot of intensity versus time for a 5% concentration sample, quenched from 70 to 25°C

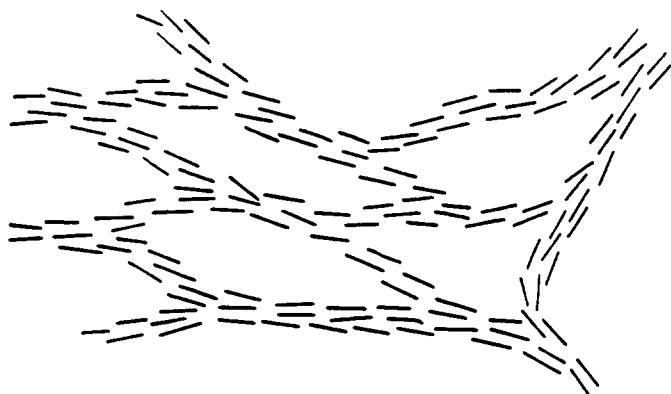


Figure 13 Model for network formed by aggregation of PBLG chains

dispersed and do not interact with each other. As the temperature is decreased, bundles of three or four chains are formed due to stacking of the side-chain benzene rings. The thermal energy driving the separation of these bundles is decreased as the temperature decreases, and attractive intermolecular forces start to dominate. In a typical benzene ring, six  $\pi$  electrons are distributed symmetrically with respect to six carbon nuclei, resulting in a sphere of positive charge on one side of the ring, and a sphere of negative charge on the other. The stacking of the side-chain benzene rings takes place because of Van der Waals attractions between these benzene rings. The diameter of a single PBLG chain is about 16 Å. Owing to the side-group packing resulting in a quasi-helix formation, three or four chains participate in the stacking process, resulting in the formation of bundles, which are about 20–25 Å in diameter. As the temperature is further decreased, aggregation of these bundles takes place, resulting in the formation of fibrils, which may contain about 5–10 bundles and are about 100 Å in diameter. The exact nature of the intermolecular forces causing the aggregation is not known. For an infinite network to be formed, these fibrils must be crosslinked. The formation of the crosslinks takes place by the branching and rejoining of different sheaf-like aggregates throughout the solution (Figure 13), resulting in an interconnected fibrillar morphology. On the scale of a few micrometres, there are inhomogeneities present, and there is a lot of space between the aggregates where there are little or no fibrils<sup>40</sup>.

The problem of the side-chain benzene rings was first considered by Elliot and Parry<sup>39</sup>. The PBLG chain has an  $\alpha$ -helix structure, with 18 residues contributing five turns of the helix, resulting in a pitch of 27 Å. Each turn therefore is 5.4 Å, and along the helix, each peptide residue translates a distance of 1.5 Å. If we considered an isolated PBLG chain, stacking of side-group benzene rings would still take place with the two participating benzene rings being 5.4 Å away from each other. Since the thickness of the benzene ring perpendicular to the ring is 3.4 Å, the benzene rings can stack only at an angle of 49° between the stack and normal to the ring. The Van der Waals attraction forces between the benzene rings are strong and they dominate the other forces present. If other chains are present, X-ray scattering work<sup>17,18,40</sup> suggests that up to four chains may participate in this stacking process, resulting in the formation of bundles.

One important question that remains to be answered is what is the nature of the intermolecular interactions

causing the bundles to aggregate, yet creating inhomogeneities over a longer length scale with a lot of space between the aggregates where there are little or no fibrils? Is crystallization the driving force for gelation? A dilute solution of rigid rods becomes metastable towards crystallization. The nature of the crystalline phase is not clear, whether it is a pure PBLG crystal, or a crystal solvate. One could then propose the following model. A dilute isotropic solution is supercooled with respect to formation of the crystal solvate phase. Isolated molecules aggregate to form clusters, which continue to aggregate. On a molecular level, polymer and solvent co-crystallize to form microfibrils, which form clusters. The clustering of clusters results in a space-spanning network having large-scale inhomogeneities<sup>37</sup>.

#### Concentrated gels

In static light scattering experiments, since the cholesteric liquid-crystalline texture is also observed in the gel phase, and the pitch is maintained in the gel phase, it appears that the twisted arrangement of molecules in the cholesteric phase is frozen by the local molecular aggregation upon gelation. Gelation appears to be a nucleation-free continuous process, by microscopy and light scattering.

For concentrated gels formed below the spinodal curve, in the unstable region, aggregation is followed by spinodal decomposition, resulting in a bicontinuous system of interpenetrating dilute and concentrated ordered regions, followed by crystallization of the polymer in the concentrated ordered phase, preventing further phase separation and resulting in an interconnected fibrillar structure. The twisted arrangement of molecules in the cholesteric phase is frozen by the local molecular aggregation upon gelation.

The gels formed between the binodal and spinodal curves in the concentrated gels are similar to the gels formed in dilute solution, where gelation is due to aggregation, and the gel is composed of clusters of microfibrils, which are distributed inhomogeneously throughout space. Local ordering of the PBLG chains is highly correlated in the form of microfibrils composed of almost parallel packed chains, resulting from a stacking of the side-chain benzene rings. Gelation results in the formation of large-scale fibrillar aggregates, the rate-determining step being diffusion.

Since PBLG is a crystallizable polymer, probably the gel junctions are of crystalline nature. In the concentrated gel, the liquid-crystalline and crystalline phases coexist. These junctions are very small crystallites, which may appear during local crystallization of the PBLG molecules.

#### SUGGESTIONS FOR FUTURE WORK

From our experiments in the ordered region, we cannot distinguish a spinodal curve. Indications are that the spinodal lies very close to the binodal curve. The nature of gels in the ordered region appears to be the same at different temperatures in the entire region, although it is very different from gels formed in the isotropic region.

The techniques we have used to study the structure and mechanism of gelation are not good enough to give us a proper understanding of what is happening at the molecular level. For this we have to look in an entirely different length scale using electron microscopy, X-ray

scattering and neutron scattering. Gelation takes place very fast on crossing the phase boundary, and some innovative experiment may have to be devised to study the kinetics of the gelation process.

There are many questions still unanswered. What is the nature of the intermolecular interactions causing the bundles to aggregate, yet creating inhomogeneities over a longer length scale with a lot of space between the aggregates where there are little or no fibrils? How close is the spinodal to the binodal in the ordered region? Wide-angle neutron scattering would be useful to understand the structure of microfibrils, whether they are composed of crystal-like paving as in the solid PBLG fibre or as in a co-crystal with solvent molecules. Is crystallization the driving force for aggregation? Small-angle neutron scattering would characterize the structure in the intermediate length scales, between that of large-scale inhomogeneities and of the microfibrils. Deuterated solvents should be used for enhanced contrast. The fractal dimension should be studied as a function of temperature and concentration<sup>37</sup>.

A better method for studying these gels with the electron microscope should be found, and studies should be extended to higher concentrations.

The kinetics of the gelation process have to be studied in more detail. We did try to study the kinetics of gelation, at different gelation temperatures, using optical microscopy, light scattering and dilatometry. Unfortunately, the results do not help us in understanding the gelation mechanism better. Some novel experimental techniques may have to be used for this study.

More computer simulations are needed to understand the diffusion-limited aggregation. In our studies, we did take into account the anisotropy of the diffusing rods, but not the orientational rearrangement of the structure. Computer simulations of diffusion-limited aggregation of semi-flexible chains, with and without orientational rearrangement, would be of tremendous interest. Future studies should involve movement of the cluster to attain the lowest possible surface energy, with the incoming rod joining the cluster where the maximum number of new bonds will be generated. This is the first step in trying to understand the mechanism of gelation. Next would be to study the cluster-cluster aggregation, many-nucleus aggregation. Future studies should include flexibility in the polymer chains and an order parameter for the rods and angular dependence between them to understand aggregation in liquid-crystalline polymers.

To compare theory and experiments, we need a better thermodynamic theory, which includes coupling between fluctuations of concentration and orientation and its effect on phase separation.

To test the one-dimensional model for spinodal decomposition and nucleation and growth, one can obtain a monodomain nematic solution of PBLG by orientation with magnetic and electric fields, and investigate the phase transition by reducing temperature<sup>37</sup>.

Finally, a theory would be very desirable which will not only explain the mechanism of gelation but also

explain the complex dynamics involved in each phase of the system.

## REFERENCES

- 1 Onsager, L. *Ann. N.Y. Acad. Sci.* 1949, **51**, 627
- 2 Flory, P. J. *Proc. R. Soc. Lond. (A)* 1956, **234**, 80
- 3 Robinson, C. *Trans. Faraday Soc.* 1955, **52**, 571
- 4 Robinson, C. *Tetrahedron* 1961, **13**, 219
- 5 Miller, W. G., Wu, L. L., Wee, E. L., Santee, G. L., Rai, J. H. and Goebel, K. D. *Pure Appl. Chem.* 1974, **38**, 37
- 6 Miller, W. G. *Annu. Rev. Phys. Chem.* 1980, **29**, 519
- 7 Wee, E. L. and Miller, W. G. *J. Phys. Chem.* 1971, **75**, 1446
- 8 Miller, W. G., Rai, J. H. and Wee, E. L. 'Liquid Crystals and Ordered Fluids' (Eds J.F. Johnson and R. S. Porter), Plenum Press, New York, 1974, p. 243
- 9 Miller, W. G., Kou, L., Tohyama, K. and Voltaggio, V. *J. Polym. Sci., Polym. Symp.* 1978, **65**, 91
- 10 Tohyama, K. and Miller, W. G. *Nature (Lond.)* 1981, **289**, 813
- 11 Russo, P. R. and Miller, W. G. *Macromolecules* 1983, **16**, 1690
- 12 Russo, P. R. and Miller, W. G. *Macromolecules* 1984, **17**, 1324
- 13 Russo, P., Magestro, P., Mustafa, M., Saunders, M. J. and Miller, W. G. *Am. Chem. Soc. Polym. Prepr.* 1986, 229
- 14 Flory, P. J. and Abe, A. *Macromolecules* 1978, **11**, 1119
- 15 Abe, A. and Flory, P. J. *Macromolecules* 1978, **11**, 1122
- 16 Flory, P. J. and Frost, R. S. *Macromolecules* 1978, **11**, 1126
- 17 Sasaki, S., Hikata, M., Shiraki, C. and Uematsu, I. *Polym. J. (Tokyo)* 1982, **14**, 205
- 18 Sasaki, S., Tokuma, K. and Uematsu, I. *Polym. Bull. (Berlin)* 1983, **10**, 539
- 19 Murthy, A. K. and Muthukumar, M. *Macromolecules* 1987, **20**, 564
- 20 Shukla, P. and Muthukumar, M. *Polym. Eng. Sci.* 1988, **28**, 1304
- 21 Koberstein, J. T. *PhD Thesis*, University of Massachusetts, Amherst, 1979
- 22 Tabar, R. J. and Stein, R. S. *J. Polym. Sci., Polym. Phys. Edn* 1982, **20**, 2041
- 23 Shukla, P. and Muthukumar, M. *J. Polym. Sci., Polym. Phys. Edn.* 1991, **29**, 1373
- 24 Russo, P. S., Karasz, F. E. and Langley, K. H. *J. Chem. Phys.* 1984, **80** (10), 15
- 25 Shukla, P., Muthukumar, M., Stein, R. S. and Langley, K. H. *J. Appl. Polym. Sci.* in press
- 26 Hermans, J. J. *J. Colloid Sci.* 1962, **17**, 638
- 27 Aoki, H., White, J. L. and Fellers, J. F. *J. Appl. Polym. Sci.* 1979, **23**, 2293
- 28 Onagi, T. and Asada, T. 'Rheology' (Eds G. Astarita, G. Marucci and L. Nicolais), Plenum Press, New York, 1980, Vol. 1
- 29 Aharoni, S. M. *Polymer* 1980, **21**, 1413
- 30 Kiss, G. and Porter, R. S. *J. Polym. Sci., Polym. Symp.* 1978, **65**, 193
- 31 Flory, P. J. 'Principles of Polymer Chemistry', Cornell University Press, Ithaca, NY, 1953
- 32 de Gennes, P. G. 'Scaling Concepts in Polymer Physics', Cornell University Press, Ithaca, NY, 1979
- 33 Hashimoto, T., Ijitsu, T., Yamaguchi, K. and Kawai, H. *Polym. J.* 1980, **12** (10), 745
- 34 Hashimoto, T., Ebisu, S., Inaba, T. and Kawai, H. *Polym. J.* 1981, **13** (7), 701
- 35 Hashimoto, T., Ebisu, S. and Kawai, H. *J. Polym. Sci.* 1981, **19**, 59
- 36 Hashimoto, T., Ebisu, S. and Kawai, H. *J. Polym. Sci., Polym. Lett. Edn* 1980, **18**, 569
- 37 Cohen, Y. *PhD Dissertation*, University of Massachusetts, Amherst, 1987
- 38 Pines, E. and Prins, W. *Macromolecules* 1973, **6**, 888
- 39 Elliot, D. and Parry, D. *J. Mol. Biol.* 1967, **25**, 1
- 40 Uematsu, I. and Uematsu, Y. *Adv. Polym. Sci.* 1984, **59**, 38